Acta Materialia 126 (2017) 401–412

Contents lists available at ScienceDirect

Acta Materialia

journal homepage: www.elsevier.com/locate/actamat

Full length article

# Damage micromechanisms in dual-phase steel investigated with combined phase- and absorption-contrast tomography

Hiroyuki Toda [a, *], Akihide Takijiri [b], Masafumi Azuma [c], Shohei Yabu [c], Kunio Hayashi [c], Dowon Seo [a], Masakazu Kobayashi [b], Kyosuke Hirayama [a], Akihisa Takeuchi [d], Kentaro Uesugi [d]

[a] Department of Mechanical Engineering, 3D/4D Structural Materials Research Centre, Kyushu University, 744, Motooka, Nishi Ward, Fukuoka City, Fukuoka 819-0395, Japan
[b] Department of Mechanical Engineering, Toyohashi University of Technology, 1-1, Hibarigaoka, Tempaku, Toyohashi City, Aichi 441-8580, Japan
[c] Steel Research Laboratories, Nippon Steel & Sumitomo Metal Corporation, 20-1 Shintomi, Futtsu City, Chiba 293-8511, Japan
[d] Japan Synchrotron Radiation Research Institute, 1-1-1, Kouto, Sayo-cho, Sayo-gun, Hyogo 679-5148, Japan

ARTICLE INFO

*Article history:*
Received 30 September 2016
Received in revised form
4 January 2017
Accepted 5 January 2017
Available online 6 January 2017

*Keywords:*
Dual-phase
Microtomography
Phase-contrast imaging
Microvoid
Ductile fracture

ABSTRACT

The single-distance phase retrieval technique was applied to contrast-enhanced imaging of the dual-phase microstructure of a ferrite/martensite dual-phase with only 1.4% difference in density between the two phases. Each high-resolution absorption-contrast image was registered with a corresponding phase-contrast image, to analyse damage evolution behaviour. The loading step at which each microvoid was nucleated was identified by tracking the microvoid throughout tension, together with its nucleation site. Premature damage initiation was observed at a relatively early stage at various nucleation sites, such as the ferrite interior, martensitic interior and ferrite/martensite interfaces; however, the subsequent growth of such microvoids was relatively moderate. On the other hand, microvoids were also initiated later due to martensitic cracking after the maximum load was reached, and these microvoids subsequently exhibited rapid growth. The martensite cracking induced additional damage evolution mainly along nearby ferrite/martensite interfaces and intersections between the martensite and the ferrite grain boundary. It is notable that the microvoids originating from martensitic cracking exhibited characteristic shear-dominated growth under macroscopic tension, whereas those originating from the other nucleation sites exhibited traditional triaxiality-dominated growth. It was concluded that the ductile fracture was dominated by the substantial force driving the growth of microvoids located on morphologically characteristic martensitic particles.



## 1. Introduction

In general, the ductile fracture process in alloys consists of nucleation, growth and coalescence of microvoids. The nucleation of microvoids is attributable to particle fracture and/or particle/matrix interfacial decohesion. It is well known that particle cracking is more apt to occur in the case of coarser particles, while interfacial decohesion is more frequently observed in the case of finer particles [1]. The ductile fracture process might also be interrelated with various microstructural heterogeneities, such as pre-existing microdefects [2,3], particle clustering [4], microstructural anisotropy [5] and dual-phase (hereinafter DP) microstructures [6–11].

It is reasonable to assume that the ductile fracture process is appreciably affected in the case of DP microstructures, especially when the deformation resistance of a harder phase is significantly higher than that of a softer matrix. A good example of such a DP microstructure is seen in DP steels that consist of a hard martensitic phase and a soft ferritic phase. In spite of extensive research activity, a variety of interpretations remain concerning the micromechanisms of damage nucleation in DP steels. The reported origins of microvoid nucleation are classified as ferrite/martensite interfacial decohesion [6–8], ferrite grain-boundary decohesion [9] and martensitic cracking [10]. It can be inferred that the reported differences among the damage micromechanisms may be partly attributable to various microstructural differences, such as

* Corresponding author.
*E-mail address:* toda@mech.kyushu-u.ac.jp (H. Toda).

http://dx.doi.org/10.1016/j.actamat.2017.01.010

martensitic volume fraction and carbon content in the martensitic phase. Each of the above-listed studies employed SEM observation of polished specimen surfaces or sections. It is interesting to note that close similarities may exist among the SEM micrographs presented as evidence for the respective damage micromechanisms advocated in the abovementioned studies. It is therefore conceivable that the different postulated damage micromechanisms might be more or less ascribed to different interpretations of an originally identical phenomenon.

With the advent of state-of-the-art imaging techniques, a thorough understanding of the detailed damage processes is expected, even when practical materials with three-dimensional (hereinafter 3D) complexity in their DP microstructures are investigated. Phase-contrast X-ray microtomography (hereinafter XMT) techniques are capable of revealing such DP microstructures with reasonable spatial resolution. For example, Landron et al. employed the X-ray holotomography technique to a DP steel, and succeeded in clearly separating the ferritic and martensitic phases at the initial unloading stage [12]. The present authors applied the single-distance phase retrieval technique to 3D observations of a DP stainless steel consisting of austenitic and ferritic phases [11,13], and found that a limited number of microvoids, initiated at later stages from fine particles located on ferrite/austenite boundaries, exhibited enormous growth, thereby inducing macroscopic ductile fracture. This was attributable to the high driving force for microvoid growth at morphologically specific ferrite/austenite boundaries. Application of this technique to the controversial interpretation of damage micromechanisms in ferrite/martensite DP steels is of great interest. In the present study, a ferrite/martensite DP steel, with a relatively coarse and interconnected martensitic phase, was evaluated as a model material.

## 2. Experimental

### 2.1. Material used

A DP steel with a chemical composition of 0.01 C, 0.1 Mn and balance iron in mass %, was prepared. A rolled plate was maintained at 1373 K for 100 s for recrystallization, followed by maintenance at 1073 K for 100 s, and then water-quenched to obtain a martensitic phase. Fig. 1 shows an optical micrograph of the investigated steel. The average volume equivalent diameter (i.e., the diameter of a sphere with volume equal to that of a non-spherical particle), and the volume fraction of martensitic particles, $V_f^M$, were 18.3 μm and 29.9%, respectively. Parallel-piped tensile specimens, which had nominal dimensions of 600 × 600 $\mu m^2$ in the gauge section, were sampled in parallel to the rolling direction, using an electro discharge machining apparatus. The gauge section was manually polished to obtain the almost circular cross-section shown below in Fig. 3.

### 2.2. 3D imaging

The XMT experiments were performed at the BL20XU beamline of SPring-8. A monochromatic X-ray beam of 37.7 keV was produced by a liquid nitrogen-cooled Si (111) double crystal monochromator. A miniature material test rig was positioned approximately 240 m from the X-ray source. The sample-to-detector distance, $L$, was 65 mm for the absorption-contrast XMT, and was varied between 200 and 800 mm for the phase-contrast XMT, for screening purposes. A CMOS camera (ORCA Flush 4.0, Hamamatsu Photonics K. K.) of 4.0 megapixels, with a 10 μm thick $Lu_2SiO_5$:Ce scintillator, was used for acquiring the projection images; and a 20 × objective lens was used to obtain an effective pixel size of 6.5 μm × 6.5 μm. Exposure time was 0.8 s. The stress-strain

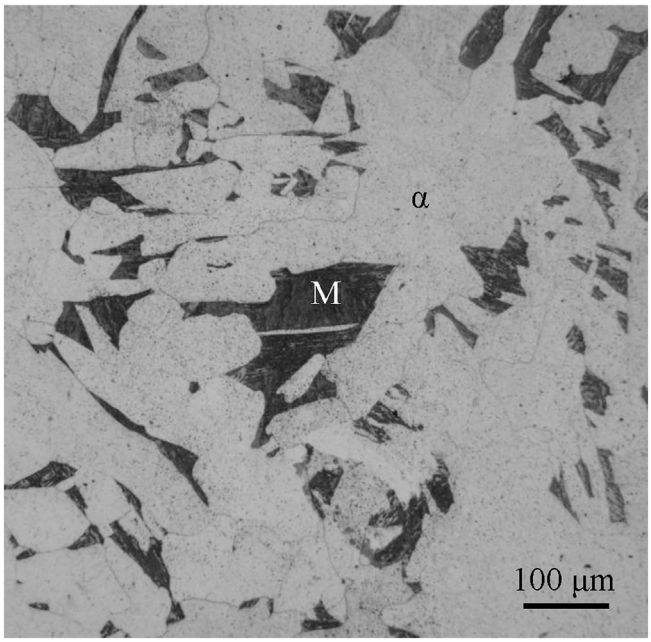


**Fig. 1.** An optical micrograph of the investigated DP steel. M and α denote the martensitic and ferritic phases, respectively.

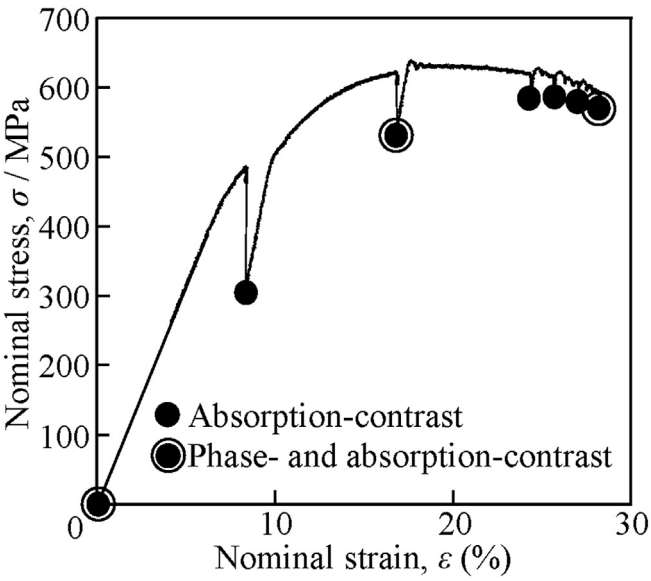


**Fig. 2.** Nominal stress - nominal strain curve obtained during the in-situ tensile test.

curve obtained during the tensile test performed at a loading rate of 0.0005 mm/s is shown in Fig. 2. The absorption-contrast XMT scans were repeated 7 times before fracture, while maintaining displacement. The phase-contrast XMT scans were obtained 3 times at the loading steps indicated in Fig. 2. The slope of the elastic part of the stress-strain-curve appears low due to small stiffness of the miniature material test rig used, which is mainly attributed to the usage of a polymer tube as a load frame instead of metallic pillars. The vertical drops in load that are observed in Fig. 2 indicate inherent relaxation behaviour of the material during the tomographic scans.

A total of 1800 and 3600 radiographs, scanning 180°, were obtained in the absorption-contrast and phase-contrast XMT scans,